



# Sliding on Slide-Ring Gels

Andrew R. Rhode<sup>1</sup> · Iván Montes de Oca<sup>2</sup> · Michael L. Chabiny<sup>c</sup> · Christopher M. Bates<sup>1,3</sup> · Angela A. Pitenis<sup>1</sup>

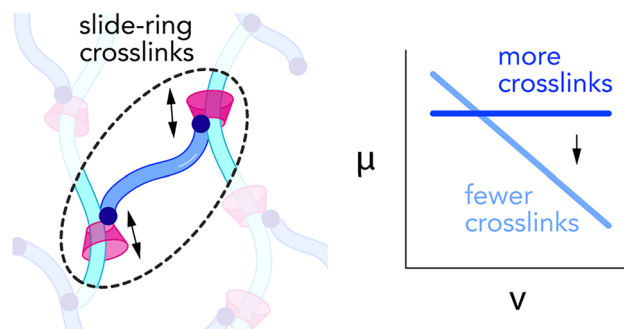
Received: 15 July 2024 / Accepted: 16 September 2024

© The Author(s) 2024

## Abstract

Recent investigations have pointed to physical entanglements that greatly outnumber chemical crosslinks as key sources of energy dissipation and low friction in hydrogel networks. Slide-ring gels are an emerging class of hydrogels described by their mobile crosslinks, which are formed by rings topologically constrained to slide along linear polymer chains within the network. These materials have enjoyed decades of study by polymer chemists but have been underexplored by the tribology community. In this work, we synthesized a pseudo-rotaxane crosslinker from poly(ethylene glycol) diacrylate (PEG-diacrylate) and  $\alpha$ -cyclodextrin-acrylate followed by hydrogel networks by connecting the sliding crosslinks with polyacrylamide chains. The mechanical and tribological properties of slide-ring hydrogels were investigated using a custom-built microtribometer. Slide-ring hydrogels exhibit unique behavior compared to conventional covalently crosslinked polyacrylamide hydrogels and offer a vast design space for future investigations.

## Graphical Abstract



**Keywords** Hydrogel · Slide-ring gel · Friction · Adhesion

## 1 Introduction

In the field of polymer chemistry, a “crosslink” is variously described as a chemical bond [1] or a noncovalent interaction [2, 3] that connects one polymer chain to another. Crosslinks within a network may also manifest as transient physical entanglements. For most elastomers and hydrogels, increasing crosslink density is generally understood to improve network strength and decrease strain-to-failure. Hydrogels are conventionally connected by covalent crosslinks, which can result in weak networks that exhibit brittle failure (Fig. 1a). With chains stretched due to swelling, static crosslinks form networks with little ability to dissipate stress [4].

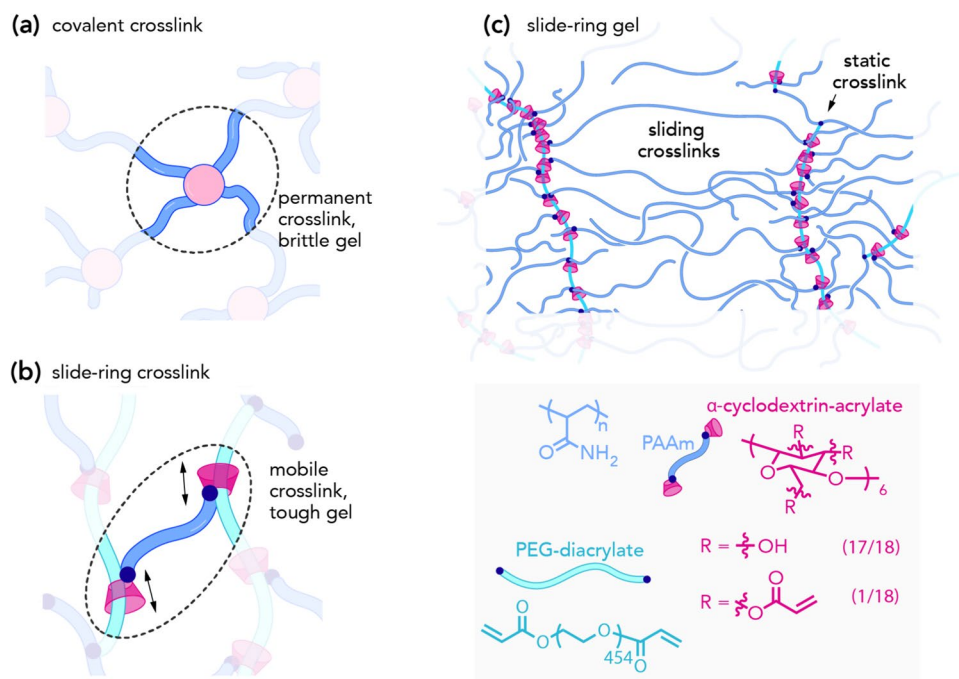
✉ Angela A. Pitenis  
apitenis@ucsb.edu

<sup>1</sup> Materials Department, University of California, Santa Barbara, Santa Barbara, CA, USA

<sup>2</sup> CICA – Centro Interdisciplinar de Química e Bioloxía and Departamento de Química, Facultade de Ciencias, Universidade da Coruña, A Coruña, 15071 A Coruña, Spain

<sup>3</sup> Department of Chemistry and Biochemistry, University of California, Santa Barbara, Santa Barbara, CA, USA

**Fig. 1** Illustrations of (a) permanent crosslinks, (b) sliding crosslinks, and (c) a hydrogel network formed by slide-ring crosslinks. Chemical composition of slide-ring crosslinker and  $\alpha$ -cyclodextrin-acrylate threaded on poly(ethylene glycol) diacrylate (PEG-diacrylate). Note that polyacrylamide (PAAm) chains connect sliding crosslinks across the network



Recent efforts by Suo and coworkers [5] have demonstrated that hydrogels formed from relatively high polymer concentrations and few covalent crosslinks exhibit high toughness, extensibility, and low friction due to a large number of physical entanglements. Topologically constrained yet mobile crosslinks have also been achieved by a variety of other network architectures including double networks [6, 7], dynamic bonds [8], and slide-rings [9]. The latter were first proposed in 1981 by the 'slip-link' model [10], in which a polymer chain slips at a trapped entanglement. In 1999, de Gennes [11] developed a theoretical model for a 'sliding gel' composed of slip-links (i.e., movable crosslinks) and unbound uncrosslinked cyclic molecules. The first slide-ring gels were not synthesized until nearly a decade later by Ito in 2007 (Fig. 1b,c) [12]. Movement of the rotaxane-based crosslinks results in sliding along polymer chains in response to applied stress that can result in substantial increases in swelling, ductility, and toughness [13].

The most studied class of slide-ring gels is based on rotaxanes made from poly(ethylene glycol) (PEG) and the readily available ring-shaped molecule  $\alpha$ -cyclodextrin [4]. When mixed in water,  $\alpha$ -cyclodextrin molecules thread over PEG chains, an interaction driven by hydrogen bonding [14]. Since PEG and  $\alpha$ -cyclodextrin are both hydrophilic, complexes of functionalized PEG and functionalized  $\alpha$ -cyclodextrin can be dissolved in water and used to crosslink hydrogels.

Many studies have established the bulk mechanical properties of PEG- and cyclodextrin-derived slide-ring gels. Ito first described the mechanics of pullulan-crosslinked polyrotaxane slide-ring gels in which cyclodextrin rings slip

along PEG chains through the 'pulley effect'. This results in a weaker scaling of modulus with crosslinker concentration than in covalently crosslinked gels, one key to the unique properties of slide-ring gels [15]. Ito and coworkers later demonstrated that increasing the crosslink density of pullulan-crosslinked polyrotaxane slide-ring gels increases stiffness without diminishing fracture toughness, in contrast with conventional structure–property relationships for covalently crosslinked hydrogels [16].

Increased chain mobility afforded by sliding crosslinks makes slide-ring gels tribologically fascinating materials. Despite the aforementioned advances in understanding the bulk mechanical properties of slide-ring gels, their tribological properties remain underexplored; to the authors' knowledge, there are no published studies on the friction of slide-ring hydrogels. Understanding the impact of sliding crosslinks on tribological properties may create new opportunities in harnessing these materials in applications ranging from flexible biosensors, biomedical devices, and water purification membranes.

In this study, slide-ring hydrogels were prepared to investigate their mechanical and tribological properties. Specifically, pseudo-rotaxane building blocks were designed where threaded polymer chains are end-capped with polymerizable groups that trap the slide-rings after network formation [17, 18]. This particular type of slide-ring hydrogel network contains a combination of sliding crosslinks as well as 'fixed' covalent crosslinks. The threaded complex of functionalized  $\alpha$ -cyclodextrin-acrylate and PEG-diacrylate used to make these gels is illustrated in Fig. 1b. This work showed that slide-ring gels have distinct tribological behavior compared

to covalently crosslinked polyacrylamide gels and provided evidence that the friction between slide-ring gels and glass is dependent on the time-dependent drainage of water away from the interface.

## 2 Materials and Methods

### 2.1 Hydrogel Synthesis

All reagents were used as received except where noted. Pseudo-rotaxane crosslinkers were synthesized from PEG-diacrylate and  $\alpha$ -cyclodextrin-acrylate through adaptations of literature protocols [17, 19, 20]. In a representative protocol, 6 g (1 equiv.) of 20 kDa PEG (Sigma-Aldrich Product #81,300) was dried under high vacuum at 35 °C overnight. The dried PEG was dissolved in 15 mL of anhydrous dichloromethane (Sigma-Aldrich Product #270,997) with 0.17 mL (4 equiv.) triethylamine (Sigma-Aldrich Product #471,283) under nitrogen with stirring. This solution was cooled to 0 °C before the addition of 0.15 mL (6 equiv.) acryloyl chloride (Sigma-Aldrich Product #549,797). The reaction then proceeded at room temperature for 24 h. The PEG-diacrylate product was collected by precipitation in cold diethyl ether.

To prepare  $\alpha$ -cyclodextrin-acrylate, 8.56 g (1 equiv.) of  $\alpha$ -cyclodextrin (Sigma-Aldrich Product #778,788) was dissolved in 125 mL of DI water with 2.97 g (6 equiv.) of potassium hydroxide (Sigma-Aldrich Product #484,016) with stirring. The reaction flask was cooled to 0 °C, and 7.15 mL (10 equiv.) of acryloyl chloride was added dropwise over 15 min. The reaction flask was brought to 40 °C for 6 h. The  $\alpha$ -cyclodextrin-acrylate was collected by precipitation in acetone following Ding et al. [19].

Both PEG-diacrylate and  $\alpha$ -cyclodextrin-acrylate were dried under high vacuum overnight after precipitation. PEG-diacrylate and  $\alpha$ -cyclodextrin-acrylate were dissolved in water individually at concentrations of 1 g per 5 mL and 1 g per 7 mL, respectively. The solutions were mixed at room temperature, then stirred at 70 °C for 90 min. The initially clear, slightly gray solutions appeared white and cloudy after equilibrating at 4 °C for one week, indicating the complexation of PEG-diacrylate and  $\alpha$ -cyclodextrin-acrylate [21] (Fig. S1). Additional evidence of complexation was the shifting and broadening of  $^1\text{H}$  NMR resonances of the complex prepared in  $\text{D}_2\text{O}$  (Fig. S2). This mixture was used directly as a pseudo-rotaxane stock solution. This ratio of  $\alpha$ -cyclodextrin-acrylate to PEG-diacrylate corresponds to a ratio of 1  $\alpha$ -cyclodextrin-acrylate molecule per 10 PEG repeat units. The maximum density possible of  $\alpha$ -cyclodextrin molecules on a PEG chain is 1  $\alpha$ -cyclodextrin molecule per two PEG repeat units [12]. Thus, a pseudo-rotaxane with one  $\alpha$ -cyclodextrin-acrylate ring per 10 PEG repeat units had a ‘coverage’ of 20% because it had 20% of

the maximum possible amount of cyclodextrin. The inherent softness and high swelling of slide-ring gels necessitated a high coverage pseudo-rotaxane at high loading to obtain hydrogel networks that permitted reproducible and reliable measurements of their mechanical and tribological properties.

Hydrogels were formed by polymerizing the pseudo-rotaxane crosslinker with acrylamide monomer. It has been previously shown that copolymerizing PEG and  $\alpha$ -cyclodextrin-based pseudo-rotaxane with acrylamide traps the  $\alpha$ -cyclodextrin rings on PEG chains, creating sliding crosslinks within the gel [17, 18]. The formation of sliding crosslinks was supported by gelation tests with varying crosslinker identities (Fig. S3). These tests showed an increase in crosslinking density resulting from the combination of PEG and  $\alpha$ -cyclodextrin-acrylate, providing evidence for the existence of sliding crosslinks in the gel. Ammonium persulfate (APS) (Sigma-Aldrich, Product #A3678) was used as a water soluble free-radical initiator with  $N,N,N',N'$ -tetramethylethylenediamine (TEMED) (Sigma-Aldrich Product #T9281) as a catalyst. Briefly, stock solutions of 50 wt.% acrylamide, 50 mg/mL APS, and 50 mg/mL TEMED were prepared in ultrapure water. The pseudo-rotaxane solution was prepared as previously described with a concentration of 154 mg/mL. Stock solutions were combined to achieve the compositions listed in Table 1. The order of addition of the stock solutions was acrylamide, water, TEMED, pseudo-rotaxane, then APS. Gels were polymerized under nitrogen (< 300 ppm  $\text{O}_2$ ) with the top surface exposed to the atmosphere to create an unmolded surface for testing. Gels were equilibrated in ultrapure water for at least one week prior to testing with multiple exchanges of the swelling media for fresh ultrapure water. All slide-ring gels increased in diameter from 12 mm initially to 20–22 mm, which corresponds to a volume increase of approximately 5× assuming isotropic swelling (Table S1). Two duplicates of each formulation were synthesized and tested. Hydrogel samples with 0.5 wt.% crosslinker were synthesized but were too soft to be accurately measured with our experimental configuration.

Since our slide-ring hydrogel system was predominantly composed of polyacrylamide, covalently crosslinked (“fixed-crosslink”) polyacrylamide hydrogels were selected as chemically similar controls. Polyacrylamide control samples were

**Table 1** Initial concentrations used in synthesizing slide-ring hydrogels

AAm (wt.%)	pseudo-rotaxane (wt.%)	APS (wt.%)	TEMED (wt.%)	Water (wt.%)
33.0	1.0	0.15	0.15	65.7
32.5	1.5	0.15	0.15	65.7

synthesized in ultrapure water at initial acrylamide concentrations of 7.5 wt.%, 12.5 wt.%, and 17.5 wt.% following the methods in Urueña et al. [22]. N,N'-Methylenebisacrylamide (MBAAm) was used as a crosslinker with the molar ratio of AAm:MBAAm equal to 200:1, and the concentrations of APS and TEMED were both 0.15 wt.%. As with the slide-ring gels, fixed-crosslink gels were polymerized under nitrogen with the top surface of the sample exposed to the atmosphere, and all samples equilibrated in ultrapure water for at least 24 h prior to testing.

## 2.2 Microindentation Measurements

A custom-built linear reciprocating tribometer was used to indent the slide-ring gels following methods previously described in Chau et al. [23] using a hemispherical borosilicate glass probe (Type 1 Class A; radius of curvature,  $R=2.6$  mm) attached to a titanium double-leaf cantilever with normal and tangential spring constants  $k_n=222.7$   $\mu\text{N}/\mu\text{m}$  and  $k_f=91.6$   $\mu\text{N}/\mu\text{m}$  to indent two flat gel disks of each formulation in three unique sites. Reduced modulus values reported for each formulation are the average and standard deviation of these repeated measurements. During indentation measurements, the hydrogel and probe were completely submerged in ultrapure water. Indentation measurements for determining  $E^*$  had constant velocity of  $v_{\text{indent}}=10$   $\mu\text{m}/\text{s}$  and a targeted normal force of  $F_n=1.0$  mN. This force corresponds to contact pressures ( $p_{\text{max}} \approx 1$  to 2 kPa) as calculated with Eq. 1:

$$p_{\text{max}} = \frac{1}{\pi} \left( \frac{6F_n(E^*)^2}{R^2} \right)^{1/3}, \quad (1)$$

where  $F_n$  is the normal force and  $E^*$  is the reduced elastic modulus. We used Eq. 2 from Hertzian contact mechanics to fit the approach curves up to  $F_n=0.5$  mN to calculate  $E^*$ :

$$F_n = \frac{4}{3} E^* R^{1/2} d^{3/2}, \quad (2)$$

where  $d$  is the depth which the probe has pushed into the gel surface. Since the instrument records  $F_n$  and  $d$ , and  $R$  is known,  $E^*$  can be calculated. To measure the contact area, the contact radius  $a$  was estimated using Eq. 3:

$$a^3 = \frac{3F_nR}{4E^*} \quad (3)$$

For fixed-crosslink gels, reduced modulus values were determined using the same protocol as for slide-ring gels but with a different probe and cantilever. The hemispherical borosilicate glass probe had a radius of curvature of  $R=3.2$  mm and the normal and tangential spring constants of the cantilever used for indentation measurements were

$k_n=61.36$   $\mu\text{N}/\mu\text{m}$  and  $k_t=75.8$   $\mu\text{N}/\mu\text{m}$ . Five indents were conducted on one location per sample. The reduced elastic modulus,  $E^*$ , used to calculate the minimum fluid film thickness,  $h_{\text{min}}$ , for fixed-crosslink polyacrylamide gels, was the averages and standard deviations of these five indentation measurements.

## 2.3 Adhesion Measurements

To investigate adhesion between the slide-ring gels and glass probe, modified indentation measurements with varying hold times at the maximum  $F_n=1.0$  mN were conducted. Indentation and retraction speeds were equal at  $v_{\text{indent}}=5$   $\mu\text{m}/\text{s}$ . After reaching the prescribed force, the probe position was held constant for maximum dwell times of  $t_{\text{dwell}}=0, 10, 60$ , or 600 s. The work of adhesion,  $W_{\text{ad}}$ , was calculated from the area above the retraction curve and below  $F_n=0$  N using Eq. 4:

$$W_{\text{ad}} = \left| \int F_n(z) dz \right|, F_n(z) < 0, \quad (4)$$

where  $z$  is the height of the glass probe in units of  $\mu\text{m}$ . The surface of the gel was set to  $z=0$ . The probe location above the gel surface corresponds to  $z>0$ , and the probe indenting the gel corresponds to  $z<0$ . One slide-ring gel sample of each formulation was indented three times in three different sites with the average and standard deviation reported for these measurements.

## 2.4 Friction Measurements

Sliding experiments were conducted using a custom-built linear reciprocating tribometer. Hydrogels were secured in a custom polyetheretherketone (PEEK) dish and submerged in ultrapure water for the duration of the experiment. The glass probes used for evaluating tribological behavior were identical in geometry to those used in the indentation measurements. Hydrogel samples were mounted to a motorized stage (Physik Instruments, L-509.20DG10, 52 mm travel range). Slide-ring gel friction was measured at sliding velocities of  $v_{\text{slide}}=10, 50$ , or 100  $\mu\text{m}/\text{s}$  across a sliding path of 6 mm (1/2 cycle). An applied normal load of  $F_n=0.5, 1$ , or 1.5 mN was maintained for at least 10 sliding cycles. The average friction coefficient of one cycle was calculated by taking the average ratio of the friction force  $F_f$  and normal force  $F_n$  in the forward and reverse directions as shown in Eq. 5:

$$\mu_{\text{cycle}} = \frac{\langle F_{f,\text{fwd}} \rangle - \langle F_{f,\text{rev}} \rangle}{2F_n}, \quad (5)$$

where  $\mu_{\text{cycle}}$  is the average friction coefficient in the free-sliding regime, which here was set to the middle 1 mm of the sliding path,  $F_{f,\text{fwd}}$  is the friction force in the forward sliding direction, and  $F_{f,\text{rev}}$  is the friction force in the reverse sliding

**Fig. 2** Representative approach and retraction curves from indentation measurements for 1.5 wt.% slide-ring crosslinker (purple) and 1.0 wt.% slide-ring crosslinker (green) following dwell times of **(a)** 0 s and **(b)** 600 s. The indentation velocity for all experiments was  $v_{\text{indent}} = 5 \mu\text{m/s}$ . The work of adhesion is indicated by the area above the indentation curve and below  $F_n = 0 \text{ N}$ . **(c)** The work of adhesion increases as a function of dwell time for both hydrogel compositions, although the 1.0 wt.% slide-ring crosslinker exhibits greater sensitivity to dwell time. Dashes are provided as guides to the eye, not fits to data

direction. Since the tribometer is configured with only one side-mounted capacitance probe to record cantilever displacements in the tangential direction, the friction force in the reverse direction is recorded as negative values.  $\mu_{\text{cycle}}$  for 10 cycles was recorded for each sample and all values of  $\mu_{\text{cycle}}$  from the same formulation and testing conditions were grouped and used to calculate the reported averages and standard deviations of friction coefficients.

Friction coefficients of the fixed-crosslink polyacrylamide gels were determined by the same procedure as the slide-ring gels except with a different probe geometry and cantilever stiffness as previously described. All tribological measurements of fixed-crosslink gels were conducted at a constant sliding velocity of 100  $\mu\text{m/s}$ . Measurements were performed at normal forces,  $F_n = 100 \mu\text{N}$ , 500  $\mu\text{N}$ , 1,000  $\mu\text{N}$ , 1,500  $\mu\text{N}$ , or 2,000  $\mu\text{N}$ . The sliding path for each fixed-crosslink gel measurement was 700  $\mu\text{m}$ . Data were collected only from experiments in which the estimated contact radius was less than 300  $\mu\text{m}$ , so that there was at least 100  $\mu\text{m}$  of free sliding in the middle of the sliding path. One measurement of the slide-ring gels resulted in a coefficient of friction below the noise floor  $\mu_{\text{noise}}$  of the instrument, calculated from Eq. 6:

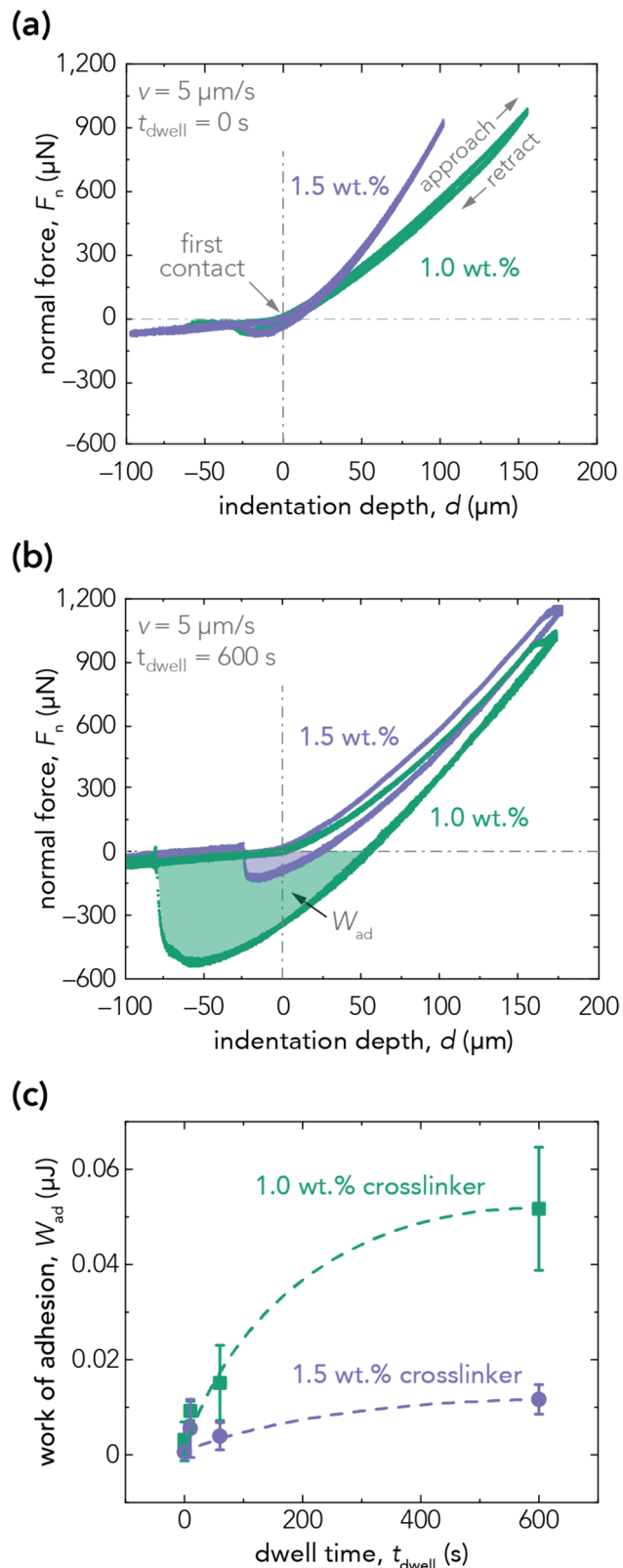
$$\mu_{\text{noise}} = \frac{F_{\text{f},\text{min}}}{F_n} = \frac{k_f x_{\text{min}}}{F_n}, \quad (6)$$

where  $k_f$  is the tangential stiffness of the cantilever ( $k_f = 437.8 \mu\text{N}/\mu\text{m}$ ) and  $x_{\text{min}}$  is the minimum displacement detectable by the capacitance probes ( $x_{\text{min}} = 5 \text{ nm}$ ). With this configuration, the experimental noise floor in friction coefficient measurements was  $\mu_{\text{noise}} = 0.001$ .

### 3 Results and Discussion

#### 3.1 Elastic Modulus Slightly Increased with Increasing Slide-Ring Crosslinker

We determined the reduced elastic moduli of the 1.0 wt.% and 1.5 wt.% crosslinked slide-ring gel formulations to be  $E^* = 10 \pm 0.9 \text{ kPa}$  and  $E^* = 15 \pm 0.4 \text{ kPa}$ , respectively, from microindentation measurements without dwell (Fig. 2a). The 1.5 wt.% crosslinked sample exhibited a greater



modulus than the 1.0 wt.% crosslinked gel, which suggests that at least some of the additional pseudo-rotaxane added to the 1.5 wt.% formulation with respect to the 1.0 wt.%

formulation did incorporate into the network, and the two formulations resulted in mechanically distinct samples.

### 3.2 Adhesion Increased with Increasing Dwell Time

Both slide-ring formulations exhibited negligible work of adhesion,  $W_{ad}$ , during indentation measurements conducted without dwelling in contact at maximum normal load,  $t_{dwell}=0$  s (Fig. 2a). Increasing dwell time resulted in significant increases in the work of adhesion for both formulations. In most cases—notably for  $t_{dwell}=60$  and 600 s—the 1.0 wt.% crosslinked sample exhibited greater  $W_{ad}$  than the 1.5 wt.% crosslinked sample (Fig. 2b,c). At maximum dwell time,  $t_{dwell}=600$  s (10 min), the work of adhesion of the 1.0 wt.% crosslinked gel ( $W_{ad}=51.7 \pm 12.9$  nJ) was approximately five times that of the 1.5 wt.% sample ( $W_{ad}=11.6 \pm 3.1$  nJ). Such sensitivity to dwell time for the 1.0 wt.% crosslinked gel suggests greater chain mobility at the surface.

### 3.3 Friction Coefficient as a Function of Sliding Speed

Friction-force traces and friction coefficients were very similar for the 1.5 wt.% crosslinked slide-ring gels when sliding velocity,  $v_{slide}$ , increased from 10 to 100  $\mu\text{m/s}$  (Fig. 3a). The friction coefficients were  $\mu=0.029 \pm 0.006$  at  $v_{slide}=10 \mu\text{m/s}$  and  $\mu=0.022 \pm 0.004$  at  $v_{slide}=100 \mu\text{m/s}$ . Friction-force traces exhibited clear separation between the forward and reverse directions for both sliding velocities, which indicated that contact was maintained between the probe and the gel surface. In contrast, the 1.0 wt.% crosslinked slide-ring gels evaluated at  $F_n=500 \mu\text{N}$  exhibited velocity-dependent friction behavior. At low sliding velocity,  $v_{slide}=10 \mu\text{m/s}$ , the friction coefficient

was relatively high ( $\mu=0.070 \pm 0.009$ ) and the presence of stick-slip in the friction-force trace was evident (Fig. 3b).

Increased adhesion at longer dwell times may provide insight into the high friction and stick-slip behavior exhibited by the 1.0 wt.% crosslinked slide-ring gels at  $v_{slide}=10 \mu\text{m/s}$ . Slow-speed sliding and quasi-static indentations both involve probes spending significant time in contact. For hydrogels, time in persistent contact could greatly exceed the polymer relaxation time and thus lead to high adhesion and hysteresis. The observations that 1.0 wt.% crosslinked gels exhibit the highest  $W_{ad}$  at the longest dwell time  $t_{dwell}=600$  s and the highest friction coefficients at the slowest sliding speeds  $v_{slide}=10 \mu\text{m/s}$  are consistent with the hypothesis that slide-ring crosslink concentration is inversely correlated with network relaxation time. Similarly,  $W_{ad}$  was only moderately sensitive to dwell time (Fig. 2c) and friction coefficients appeared mostly insensitive to sliding velocity (Fig. 3c) for the 1.5 wt.% crosslinked gel. At the slowest sliding velocity,  $v_{slide}=10 \mu\text{m/s}$ , the 1.5 wt.% crosslinked samples exhibited lower friction coefficients than the 1.0 wt.% crosslinked samples. This agrees with adhesion trends: the 1.5 wt.% crosslinked sample moderately increased  $W_{ad}$  at longer dwell times but increased to a much lesser extent than the 1.0 wt.% crosslinked sample. Differences in the work of adhesion and slow-speed friction may be related to changes in reduced elastic moduli,  $E^*$ , between the 1.0 wt.% and 1.5 wt.% crosslinked samples. The projected contact area (estimated from Eq. 3) of the moderately softer 1.0 wt.% sample under an applied load of  $F_n=1,000 \mu\text{N}$  is about 130% of the contact area of the 1.5 wt.% crosslinked sample. However, contact area differences likely do not fully account for the roughly 500% difference in adhesion at the highest dwell time or the significant difference in friction coefficient at the slowest sliding speed.

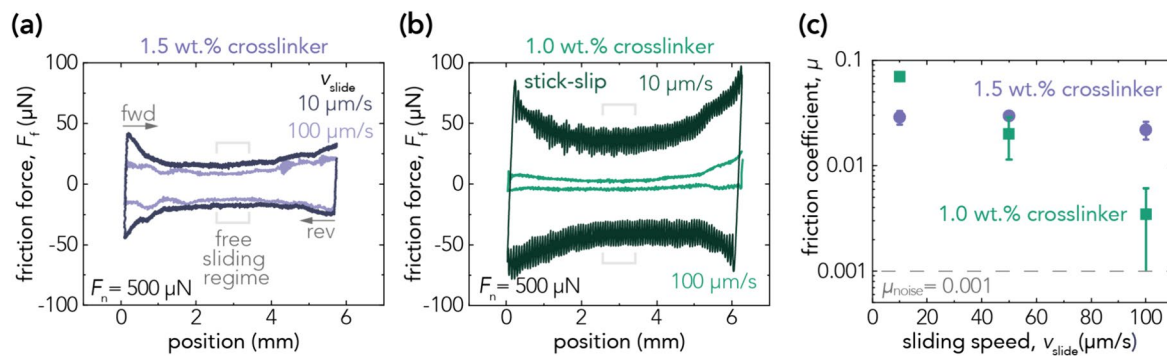


**Fig. 3** Representative friction-force measurements of (a) 1.5 wt.% slide-ring crosslinker and (b) 1.0 wt.% slide-ring crosslinker as a function of position over a single reciprocating cycle for 10  $\mu\text{m/s}$  and 100  $\mu\text{m/s}$  sliding velocities. (c) Average friction coefficient as a function of sliding speed for two hydrogel compositions. Error bars represent the standard deviation of friction coefficient measurements over 10 reciprocating cycles per experiment for two independent hydrogel samples. The noise floor in friction coefficient measurements is  $\mu_{noise}=0.001$

sent the standard deviation of friction coefficient measurements over 10 reciprocating cycles per experiment for two independent hydrogel samples. The noise floor in friction coefficient measurements is  $\mu_{noise}=0.001$

### 3.4 Mobility and Lubricity

Slide-ring gels represent a class of materials with low modulus and potentially greater capacity for energy dissipation than conventional (fixed-crosslink) polyacrylamide hydrogels. Both slide-ring gel formulations exhibited  $E^* < 20$  kPa. The 7.5 wt.%, 12.5 wt.%, and 17.5 wt.% fixed-crosslink polyacrylamide gels spanned reduced elastic moduli of  $E^* = 40 \pm 1$  kPa,  $E^* = 136 \pm 8$  kPa, and  $E^* = 226 \pm 9$  kPa, respectively. The friction coefficient,  $\mu$ , generally increased with reduced elastic modulus,  $E^*$ , for both slide-ring and covalently (fixed) crosslinked hydrogels (Fig. 4a). The incorporation of sliding crosslinks is one route to increase mobility in hydrogel networks and achieve both low modulus and low friction. The possibility of dangling chains at the sliding interface may also contribute to lubricity as well as higher adhesion at long dwell times [24].

### 3.5 Considerations of Soft EHL

At the highest sliding velocity and lowest applied force,  $v_{\text{slide}} = 100 \mu\text{m/s}$  and  $F_n = 500 \mu\text{N}$ , the average friction coefficient was  $\mu = 0.003 \pm 0.003$  for the 1.0 wt.% crosslinked sample (Fig. 3c). This calculation included data points at the noise floor of friction coefficient measurements,  $\mu \approx 0.001$ . Trends in adhesion measurements do not explain the extremely low friction of the 1.0 wt.% crosslinked samples at the highest sliding speed,  $v_{\text{slide}} = 100 \mu\text{m/s}$ ; both slide-ring gel formulations exhibited similarly low work of adhesion,

$W_{\text{ad}}$ , for short dwell times ( $t_{\text{dwell}} = 0$  s or 10 s) yet resulted in significant differences in friction coefficient,  $\mu$ , for the highest sliding speed, which suggests another mechanism dominates. In the fast-sliding velocity measurement for the 1.0 wt.% crosslinked slide-ring gel, there was no apparent separation between the forward and reverse directions of the friction-force traces, which may be evidence of fluid film entrainment.

To investigate the extent to which low friction coefficients could be due to fluid film lubrication, Eq. 7 was used to calculate the minimum fluid film thickness,  $h_{\text{min}}$  [25, 26] to achieve soft elasto-hydrodynamic lubrication (EHL).

$$h_{\text{min}} = 2.8R^{0.77}(\eta_0 v_{\text{slide}})^{0.65}(E^*)^{-0.44}(F_n)^{-0.21}, \quad (7)$$

where  $\eta_0$  is the viscosity of the fluid (water,  $\eta_0 = 8.9 \times 10^{-4} \text{ Pa}\cdot\text{s}$ ) across the interface,  $v_{\text{slide}}$  is the sliding velocity,  $E^*$  is the reduced elastic modulus of the sample, and  $F_n$  is the applied normal force.

Increasing fluid film layer thickness with increasing sliding velocity,  $v_{\text{slide}}$ , is a reasonable explanation for the failure of adhesion measurements to predict the difference in friction between the 1.0 wt.% and 1.5 wt.% crosslinked slide-ring gels. Fluid films may have partially separated the sliding interfaces at high  $v_{\text{slide}}$ , but not for brief dwell times,  $t_{\text{dwell}}$ . Slide-ring gels generally showed decreasing friction coefficients,  $\mu$ , with increasing  $h_{\text{min}}$ , the estimated minimum fluid film thickness (Fig. 4b). The 1.0 wt.% crosslinked formulation had a stronger dependence on  $h_{\text{min}}$  than the 1.5 wt.%

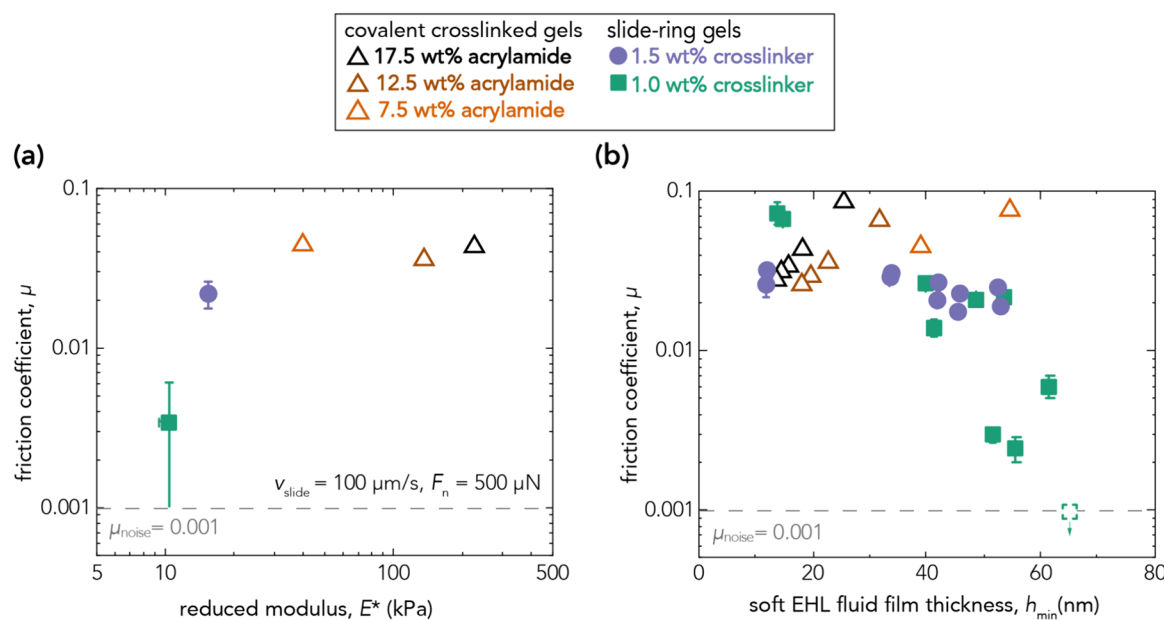


**Fig. 4** Comparisons among hydrogels with slide-ring and fixed crosslinks. (a) Slide-ring hydrogels generally exhibit lower friction coefficients,  $\mu$ , and smaller reduced elastic moduli,  $E^*$ , than fixed-

crosslink hydrogels. (b) Slide-ring hydrogels may achieve lower friction coefficients than conventionally crosslinked polyacrylamide hydrogels by facilitating conditions for soft EHL fluid film formation

crosslinked formulation. In contrast, covalently crosslinked hydrogels exhibited increased friction coefficients with larger  $h_{\min}$ .

If the combined surface roughness of the probe and gel is less than  $h_{\min}$  then the probe may slide on a fluid film layer rather than the gel itself. However, friction-force traces were evaluated for all experiments, and in all but one case (the 1.0 wt.% slide-ring crosslinker at highest sliding velocity), there was clear separation between  $F_{f,fwd}$  and  $F_{f,rev}$  as well as symmetric lateral contact stiffness at the reversals, all which suggest that physical contact was maintained between the probe and gel surfaces for the duration of each sliding cycle. For the single measurement below the noise floor that was previously discussed, no separation was observed between  $F_{f,fwd}$  and  $F_{f,rev}$ . The lack of separation between forward and reverse friction-force traces is evidence that the probe may have been sliding on a fluid film. The corresponding  $h_{\min} = 65$  nm for this measurement (indicated by a dashed green square in Fig. 4b) was the largest  $h_{\min}$  estimated across all experiments, which supports the idea that fluid film lubrication is beginning to occur.

Although the soft EHL calculations in this investigation only provide theoretical estimates,  $h_{\min}$  remains a valuable parameter that helps describe situations in which fluid film lubrication is more likely to occur (increased  $v_{\text{slide}}$ , decreased  $E^*$ , and decreased  $F_n$ ). The use of  $h_{\min}$  conveniently encompasses all the changes in sliding conditions applied to the slide-ring gels in this study. The stronger dependence of friction on  $h_{\min}$  in the 1.0 wt.% crosslinked slide-ring gels with respect to the 1.5 wt.% crosslinked gels can be understood in the context of the adhesion measurements in Fig. 3. Compared to the 1.5 wt.% crosslinked gel, the 1.0 wt.% crosslinked gel was more adhesive at long dwell times and had higher friction at  $v_{\text{slide}} = 10 \mu\text{m/s}$ . Increasing  $h_{\min}$  by increasing  $v_{\text{slide}}$ , decreasing  $E^*$ , or decreasing  $F_n$  would have removed some of these adhesive contacts between the probe and the gel in exchange for contact between the probe and a lubricating layer of water. This likely had a greater impact on the friction of the 1.0 wt.% crosslinked gel due to the increased adhesion between the 1.0 wt.% gel and the glass probe. Furthermore, for high values of  $h_{\min}$ , in which there was low contact area between the gel and probe, an incremental increase in  $h_{\min}$  would result in a greater percentage reduction in contact area.

### 3.6 Time-Dependent Drainage

Friction between the glass probe and the pseudo-rotaxane gels may proceed through mechanisms of polymer relaxation leading to interfacial drainage (Fig. 5). Dunn et al. hypothesized that friction of hydrogels with soft surface gel layers ( $E^* \approx 25 \text{ kPa}$ ) increased with increasing force because the probe crushed the surface gel layer, forcing water out

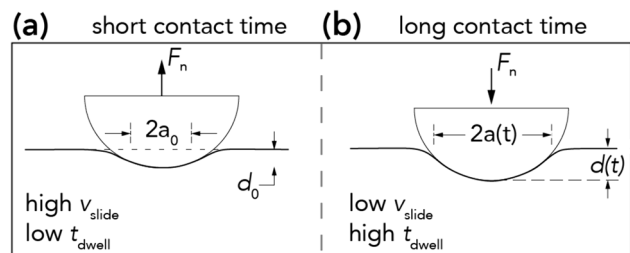


**Fig. 5** Schematic depicting (a) short contact times and (b) long contact times between hemispherical glass probes and slide-ring hydrogels during friction and indentation measurements. The contact area likely grows under low sliding speeds and high dwell times, which contributes to higher work of adhesion and higher friction coefficients for the softer slide-ring hydrogel (1.0 wt.% crosslinker)

of the contact interface and creating a region of high polymer density at the surface of the gel [27]. In this work, it is unlikely that the applied normal loads led to contact pressures sufficient to collapse the gels. Instead of drainage due to increased force, drainage may proceed due to increased time, facilitating greater adhesion between the probe and gel. As the polymer network remained in persistent contact with the probe, relaxations in the polymer may have preferentially drive water away from regions of higher osmotic pressure to regions of lower osmotic pressure, away from the contacting or sliding interface. Higher polymer density may thus have led to higher friction at slower sliding speeds and lower values of  $h_{\min}$ . This hypothesis is supported by the work of Schulze et al. which showed that the increase in adhesion with longer dwell times was due to polymer network relaxations when the applied pressure was less than the osmotic pressure of the gel [28].

## 4 Concluding Remarks

Slide-ring hydrogels were prepared with 0.5 wt.%, 1.0 wt.%, and 1.5 wt.% pseudo-rotaxane crosslinkers formed from  $\alpha$ -cyclodextrin-acrylate mobile rings threaded around PEG-diacrylate chains connected by polyacrylamide. The mechanical and tribological properties of each slide-ring hydrogel formulation were characterized with a custom-built microtribometer for indentation and linear reciprocating sliding experiments, respectively. Although the 0.5 wt.% crosslinker samples were too soft and slippery for reliable measurements above the experimental noise floor, slide-ring hydrogels with 1.0 wt.% and 1.5 wt.% crosslinker exhibited low reduced elastic modulus ( $E^* < 20 \text{ kPa}$ ), low adhesion at short dwell times ( $t_{\text{dwell}} = 0 \text{ s}$ ), and generally low friction at moderate sliding speeds ( $0.02 < \mu < 0.03$  at  $v_{\text{slide}} = 50 \mu\text{m/s}$ ). However, 1.0 wt.% crosslinked slide-ring gels exhibited velocity-dependent friction behavior

as well as dwell-time-dependent adhesion. This may be due to increased chain mobility at the surface leading to higher fluid film thickness ( $h_{\min} = 65$  nm) even at a sliding velocity generally considered slow in engineering applications,  $v_{\text{slide}} = 100$   $\mu\text{m/s}$ . The 1.0 wt.% crosslinker composition also results in stick-slip at the lowest sliding velocity,  $v_{\text{slide}} = 10$   $\mu\text{m/s}$ . The results of this investigation point to slide-ring gels as a class of hydrogels distinct from conventional hydrogels with fixed, covalent crosslinks. Slide-ring gels offer a vast design space for creating water-borne materials with unique mechanical and tribological behavior tailored for specific engineering applications, from biomedical devices to soft robotics.

**Supplementary Information** The online version contains supplementary material available at <https://doi.org/10.1007/s11249-024-01920-x>.

**Acknowledgements** The authors gratefully acknowledge Dr. Allison L. Chau for providing experimental data for covalently crosslinked polyacrylamide hydrogels and the members of the Interfacial Engineering Laboratory, the Bates Laboratory, and the Chabinyc Laboratory for their support. Special thanks to Prof. Craig Hawker for his thoughtful suggestions on the chemistry of slide-ring gels, and to Prof. Baskar Ganapathysubramanian and Prof. Adarsh Krishnamurthy from Iowa State University for valuable discussions.

**Author Contributions** A.R.R., M.L.C., C.M.B., and A.A.P. designed the study. A.R.R. and I.M.D.O. synthesized samples, A.R.R. conducted tribological measurements, and all authors analyzed the results. A.R.R. and A.A.P. wrote the main text of the manuscript with input from all authors and prepared figures. All authors reviewed and approved the manuscript.

**Funding** This work was supported by the DMREF Program of the National Science Foundation under Award No. 2323715. The MRL Shared Experimental Facilities are supported by the MRSEC Program of the NSF under Award No. DMR 2308708; a member of the NSF-funded Materials Research Facilities Network ([www.mrfn.org](http://www.mrfn.org)). This work was partially supported by the BioPACIFIC Materials Innovation Platform of the National Science Foundation under Award No. DMR-1933487. A.R.R. acknowledges support from the NSF Graduate Research Fellowship Program under Grant No. 2139319.

**Data Availability** Data are available free of charge from the Dryad repository at: <https://doi.org/10.5061/dryad.ksn02v7dv>.

## Declarations

**Conflict of interest** The authors declare no competing interests.

**Open Access** This article is licensed under a Creative Commons Attribution 4.0 International License, which permits use, sharing, adaptation, distribution and reproduction in any medium or format, as long as you give appropriate credit to the original author(s) and the source, provide a link to the Creative Commons licence, and indicate if changes were made. The images or other third party material in this article are included in the article's Creative Commons licence, unless indicated otherwise in a credit line to the material. If material is not included in the article's Creative Commons licence and your intended use is not permitted by statutory regulation or exceeds the permitted use, you will need to obtain permission directly from the copyright holder. To view a copy of this licence, visit <http://creativecommons.org/licenses/by/4.0/>.

## References

1. Wichterle, O., Lím, D.: Hydrophilic gels for biological use. *Nature* **185**, 117–118 (1960). <https://doi.org/10.1038/185117a0>
2. Eagland, D., Crowther, N.J., Butler, C.J.: Complexation between polyoxyethylene and polymethacrylic acid—the importance of the molar mass of polyoxyethylene. *Eur. Polym. J.* **30**, 767–773 (1994). [https://doi.org/10.1016/0014-3057\(94\)90003-5](https://doi.org/10.1016/0014-3057(94)90003-5)
3. Gacesa, P.: Alginates. *Carbohydr. Polym.* **8**, 161–182 (1988). [https://doi.org/10.1016/0144-8617\(88\)90001-X](https://doi.org/10.1016/0144-8617(88)90001-X)
4. Zhao, X., Chen, X., Yuk, H., et al.: Soft materials by design: unconventional polymer networks give extreme properties. *Chem. Rev.* **121**, 4309–4372 (2021). <https://doi.org/10.1021/acs.chemrev.0c01088>
5. Kim, J., Zhang, G., Shi, M., Suo, Z.: Fracture, fatigue, and friction of polymers in which entanglements greatly outnumber cross-links. *Science* **374**, 212–216 (2021). <https://doi.org/10.1126/science.abg6320>
6. Gong, J.P.: Why are double network hydrogels so tough? *Soft Matter* **6**, 2583–2590 (2010). <https://doi.org/10.1039/B924290B>
7. Means, A.K., Shrode, C.S., Whitney, L.V., et al.: Double network hydrogels that mimic the modulus, strength, and lubricity of cartilage. *Biomacromol* **20**, 2034–2042 (2019). <https://doi.org/10.1021/acs.biomac.9b00237>
8. Nimmo, C.M., Owen, S.C., Shoichet, M.S.: Diels–Alder click cross-linked hyaluronic acid hydrogels for tissue engineering. *Biomacromol* **12**, 824–830 (2011). <https://doi.org/10.1021/bm101446k>
9. Zheng, S.Y., Liu, C., Jiang, L., et al.: Slide-ring cross-links mediated tough metallosupramolecular hydrogels with superior self-recoverability. *Macromolecules* **52**, 6748–6755 (2019). <https://doi.org/10.1021/acs.macromol.9b01281>
10. Ball, R.C., Doi, M., Edwards, S.F., Warner, M.: Elasticity of entangled networks. *Polymer* **22**, 1010–1018 (1981). [https://doi.org/10.1016/0032-3861\(81\)90284-6](https://doi.org/10.1016/0032-3861(81)90284-6)
11. de Gennes, P.-G.: Sliding gels. *Phys. Stat. Mech. Its. Appl.* **271**, 231–237 (1999). [https://doi.org/10.1016/S0378-4371\(99\)00227-7](https://doi.org/10.1016/S0378-4371(99)00227-7)
12. Ito, K.: Novel cross-linking concept of polymer network: synthesis, structure, and properties of slide-ring gels with freely movable junctions. *Polym. J.* **39**, 489–499 (2007). <https://doi.org/10.1295/polymj.PJ2006239>
13. Noda, Y., Hayashi, Y., Ito, K.: From topological gels to slide-ring materials. *J. Appl. Polym. Sci.* (2014). <https://doi.org/10.1002/app.40509>
14. Lin, Q., Li, L., Tang, M., et al.: Rapid macroscale shape morphing of 3D-printed polyrotaxane monoliths amplified from pH-controlled nanoscale ring motions. *J. Mater. Chem. C* **6**, 11956–11960 (2018). <https://doi.org/10.1039/C8TC02834F>
15. Ito, K.: Novel entropic elasticity of polymeric materials: why is slide-ring gel so soft? *Polym. J.* **44**, 38–41 (2012). <https://doi.org/10.1038/pj.2011.85>
16. Liu, C., Kadono, H., Mayumi, K., et al.: Unusual fracture behavior of slide-ring gels with movable cross-links. *ACS Macro Lett.* **6**, 1409–1413 (2017). <https://doi.org/10.1021/acsmacrolett.7b00729>
17. Feng, L., Jia, S.-S., Chen, Y., Liu, Y.: Highly elastic slide-ring hydrogel with good recovery as stretchable supercapacitor. *Chem. Eur. J.* **26**, 14080–14084 (2020). <https://doi.org/10.1002/chem.202001729>
18. Wang, S., Chen, Y., Sun, Y., et al.: Stretchable slide-ring supramolecular hydrogel for flexible electronic devices. *Commun. Mater.* **3**, 1–9 (2022). <https://doi.org/10.1038/s43246-022-00225-7>
19. Ding, L., Li, Y., Jia, D., et al.:  $\beta$ -Cyclodextrin-based oil-absorbents: preparation, high oil absorbency and reusability. *Carbohydr. Polym.* **83**, 1990–1996 (2011). <https://doi.org/10.1016/j.carbpol.2010.11.005>

20. Fleury, G., Brochon, C., Schlatter, G., et al.: Synthesis and characterization of high molecular weight polyrotaxanes: towards the control over a wide range of threaded  $\alpha$ -cyclodextrins. *Soft Matter* **1**, 378–385 (2005). <https://doi.org/10.1039/B510331B>
21. Ceccato, M., Lo, N.P., Baglioni, P.:  $\alpha$ -cyclodextrin/polyethylene glycol polyrotaxane: a study of the threading process. *Langmuir* **13**, 2436–2439 (1997). <https://doi.org/10.1021/la9609231>
22. Urueña, J.M., Pitenis, A.A., Nixon, R.M., et al.: Mesh size control of polymer fluctuation lubrication in gemini hydrogels. *Biotribology* **1–2**, 24–29 (2015). <https://doi.org/10.1016/j.biотri.2015.03.001>
23. Chau, A.L., Getty, P.T., Rhode, A.R., et al.: Superlubricity of pH-responsive hydrogels in extreme environments. *Front. Chem.* **10**, 891519 (2022)
24. Hasan, M.M., Dunn, A.C.: Fewer polymer chains but higher adhesion: how gradient-stiffness hydrogel layers mediate adhesion through network stretch. *J. Chem. Phys.* **159**, 184706 (2023). <https://doi.org/10.1063/5.0174530>
25. Hamrock, B.J., Dowson, D.: Elastohydrodynamic lubrication of elliptical contacts for materials of low elastic modulus I—fully flooded conjunction. *J. Lubr. Technol.* **100**, 236–245 (1978). <https://doi.org/10.1115/1.3453152>
26. Rennie, A.C., Dickrell, P.L., Sawyer, W.G.: Friction coefficient of soft contact lenses: measurements and modeling. *Tribol. Lett.* **18**, 499–504 (2005). <https://doi.org/10.1007/s11249-005-3610-0>
27. Dunn, A.C., Urueña, J.M., Huo, Y., et al.: Lubricity of surface hydrogel layers. *Tribol. Lett.* **49**, 371–378 (2005). <https://doi.org/10.1007/s11249-012-0076-8>
28. Schulze, K.D., Hart, S.M., Marshall, S.L., et al.: Polymer osmotic pressure in hydrogel contact mechanics. *Biotribology* **11**, 3–7 (2017). <https://doi.org/10.1016/j.biотri.2017.03.004>

**Publisher's Note** Springer Nature remains neutral with regard to jurisdictional claims in published maps and institutional affiliations.